Bachelor thesis
Using the nitrogen surface abundance as a clock in massive main sequence stars

Mikolaj Borzyszkowski

angefertigt im
Argelander Institut für Astronomie

vorgelegt der
Mathematisch-Naturwissenschaftlichen Fakultät der Universität Bonn

June 2010

1.Gutachter: Professor Dr. Norbert Langer
2.Gutachter: Professor Dr. Pavel Kroupa

Abstract

In this bachelor thesis evolutionary models of massive main sequence stars including a theory of rotational mixing are used to derive expressions for the evolution of the surface nitrogen abundance with time, mass and rotational velocity. The aim is to set up a method which uses the nitrogen surface abundance to constrain the stellar age. The new method is applied to observational data of the VLT-FLAMES Survey of Massive Stars and the resulting age constraints are compared with ages estimated by fitting isochrones in the Hertzsprung-Russel-Diagram.
We find a group of nitrogen poor and fast rotating stars which are in conflict with their age prediction through the measured nitrogen abundance and the age estimate with isochrones in the HR diagram.

Contents

1 Introduction

Although massive stars have a short lifetime compared to lower mass stars they are important for the evolution of the universe. Only in massive stars heavy elements up to iron can be produced by nuclear fusion which now take influence in the evolution of all stars as metallicity. In the early universe massive stars are believed to play an important role in the re-ionization of the universe as population III stars, [Haiman & Loeb, 1997]. Due to their strong influence on the evolution of the universe it is important to understand the evolution of massive stars. Initial mass and metallicity were for a long time considered to be the primary parameters determining the evolution of a star, but additionally the rotation of stars was found to play an important role especially in the evolution of massive stars. Stellar rotation can drive various processes in the stellar interior like large scale circulations or shear instabilities, [Endal & Sofia, 1978], which are believed to raise the main sequence lifetime of a star by providing hydrogen from the envelope to the core hydrogen burning region during the main sequence evolution. At the end of their life massive rotating stars can explode in a bright supernova and are candidates for gamma-ray bursts [Yoon et al., 2006], which are objects observed at highest redshift. The initial rotation velocity is therefore an essential parameter of the star and it is a fundamental issue to understand the effects of rotation.

In this thesis, a special look is taken to rotational induced mixing processes in massive stars especially to the nitrogen surface abundance. In massive stars, hydrogen is fused into helium via the CNO cycle. In this fusion cycle the protons fuses with the carbon and nitrogen, which the star contains due to the metallicity, to oxygen ^{15}O which decays first to ^{15}N which mostly decays in the α mode and emits an helium core. The remaining carbon then fuses again with protons to nitrogen and oxygen which decays again. So the effect is that from four hydrogen cores one helium core is produced while the summarized amount of carbon, nitrogen and oxygen is constant. Since the fusion of ^{14}N and a proton to ^{15}O has the lowest possibility in stellar cores the amount of nitrogen rises in the core relative to carbon and oxygen until the reaction cycle is in equilibrium. This overdencity of nitrogen in the core is transported to the surface of the stars and enriches the envelope by rotational induced mixing processes [Heger & Langer, 2000].

Using a stellar evolution code including rotational mixing, [Brott et al., 2010a] simulated stars with different initial mass, metallicity and initial rotation velocity. They provided three evolution grids of stars characterized by different metallicities, which are equal to the metallicity of the Milky Way close to the Sun (MW), the Large Magellanic Cloud (LMC), and the Small Magellanic Cloud (SMC).

In previous work the measured nitrogen abundance of stars was compared with predictions from such model grids. [Hunter et al., 2008a] and [Brott et al., 2010b] found a large fraction of stars of the VLT-FLAMES survey of Massive Stars that agrees in their nitrogen abundance with the prediction of the stellar evolution model. But they also identified two peculiar groups of stars in the sample of the VLT-FLAMES survey: the first characterized by a nitrogen enriched surface and slow rotation, and the second by a nitrogen poor surface and fast rotation. Both groups can not be explained by the current theory of rotational induced mixing.

In this thesis the grids presented in [Brott et al., 2010a] will be used to derive expressions for the nitrogen surface abundance as function of time, mass and rotation velocity (Sect.2). A new method of constraining the age of a star due to its nitrogen surface abundance will be presented and applied to data obtained in the VLT-FLAMES survey (Sect.3.1). Nitro-

gen is the element of choice because in contrast to for example carbon the nitrogen amount in the star is rising in the hydrogen burning phase in massive stars. Moreover the mixing of nitrogen is efficient which makes it easier to distinguish an enrichment in observations. Since the enrichment of nitrogen is monotonies in the model an age estimation is possible [Brott et al., 2010b]. Additionally the age of the observed stars will be estimated with fitting isochrones in the Hertzsprung-Russel-Diagram (Sect.3.2) and compared to the result of the age constraint due to nitrogen surface abundance to test if the theory of rotational mixing is able to predict stellar ages (Sect.4). With this new method of testing the model of rotational mixing this work is able to provide independent results to previous work. It is not needed to make further assumptions on the stellar population of the LMC, SMC, or MW which makes it possible test the theory of rotational mixing directly through the stellar evolution grids.

2 Nitrogen surface abundance as function of time in stellar models

The main sequence (MS) lifetime of stars depends sensitively on their mass. Therefore the fraction of the main sequence life time τ is used as the independent time variable for the nitrogen surface abundance $\mathcal{N} = \log\left(\frac{\mathrm{N}}{\mathrm{H}}\right) + 12$, where $\frac{\mathrm{N}}{\mathrm{H}}$ is the ratio of nitrogen to hydrogen. The abundance $\mathcal{N}$ is then normalized to a hydrogen abundance of $\mathcal{H} = 12$ dex. So $\mathcal{N}$ expresses the logarithmic number of nitrogen per 10^{12} hydrogen atoms. The used stellar evolution grids have two parameters for the stars: the initial rotation velocity V_{init} and the initial mass M with which the stellar models are initialized. In Fig.1 the evolution of the surface abundance of stars of the stellar evolution grid is presented for different initial masses and initial rotational velocity. The nitrogen abundance starts to rise at a certain time and gets into saturation. The nitrogen surface abundance is a strong function of the initial rotational velocity. It also depends on the mass of the star but the change with mass is not as strong as with rotational velocity.

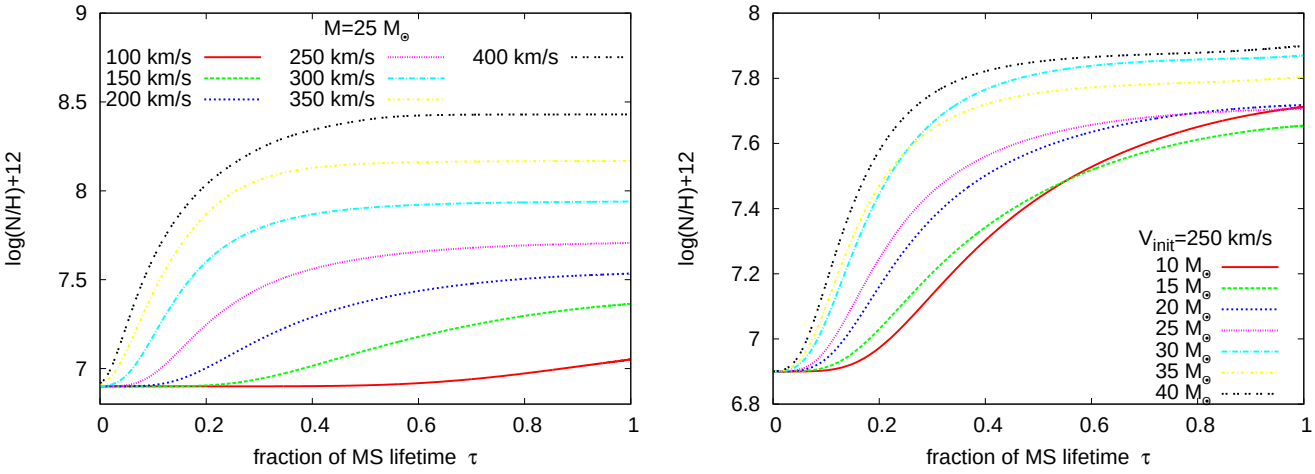

Figure 1: Evolution of the nitrogen surface abundance $\mathcal{N}$ as function of the fraction of the main sequence lifetime τ for different models of the stellar evolution grid at LMC metallicity. Left panel: Stellar models with constant initial mass $M = 25\mathrm{M}_{\odot}$ and different initial rotation velocity V_{init} written in the figure key. Right panel: Stellar models with constant initial rotation velocity $V_{\mathrm{init}} = 250\frac{\mathrm{km}}{\mathrm{s}}$ and different initial mass M written in the figure key.

2.1 Determining the velocity and mass dependence

The shape of the nitrogen surface abundance is asymmetric and monotonies rising with a plateau at high fraction of the main sequence lifetime τ. A good function providing these properties to describe the nitrogen surface abundance is

$$\mathcal{N}(\tau) = a + c \cdot \gamma_d(b \cdot \tau), \tag{1}$$

where a, b, c, d depend on V_{init} and M and γ is the incomplete gamma function. The incomplete gamma function $\gamma_d(b \cdot \tau)$ depends on $b \cdot \tau$ and the parameter d. In the present thesis the incomplete gamma function is normalized with the complete gamma function Γ to

$$\gamma_d(b \cdot \tau) = \frac{1}{\Gamma(d)} \int_0^{b \cdot \tau} x^{d-1} e^{-x} dx, \tag{2}$$

so the values of the incomplete gamma function are $\gamma \epsilon [0:1]$ which means that only the parameter c is responsible for the hight of the curve. Furthermore one can note since $\gamma_d(0) = 0$, a is the initial nitrogen abundance which is independent of initial mass and rotation velocity. For the LMC, $a = 6.9$ for example. In Fig.1 it can be seen that with higher rotation velocity significant enrichment of nitrogen at the surface happens earlier in the main sequence evolution, what the parameter b is for in Eq.(1). Now parameter d is left and in fact Eq.(1) is overdetermined in d. Therefore we have to assign d a value. From fitting Eq.(1) to the stellar evolution grid data it turns out that with setting d to

$$d = 9 - \frac{V_{\rm init}}{50} \tag{3}$$

Eq.(1) is able to reproduce the shape of the enrichment of the the nitrogen surface abundance well. This relation is used for the LMC, the SMC and the MW grid.

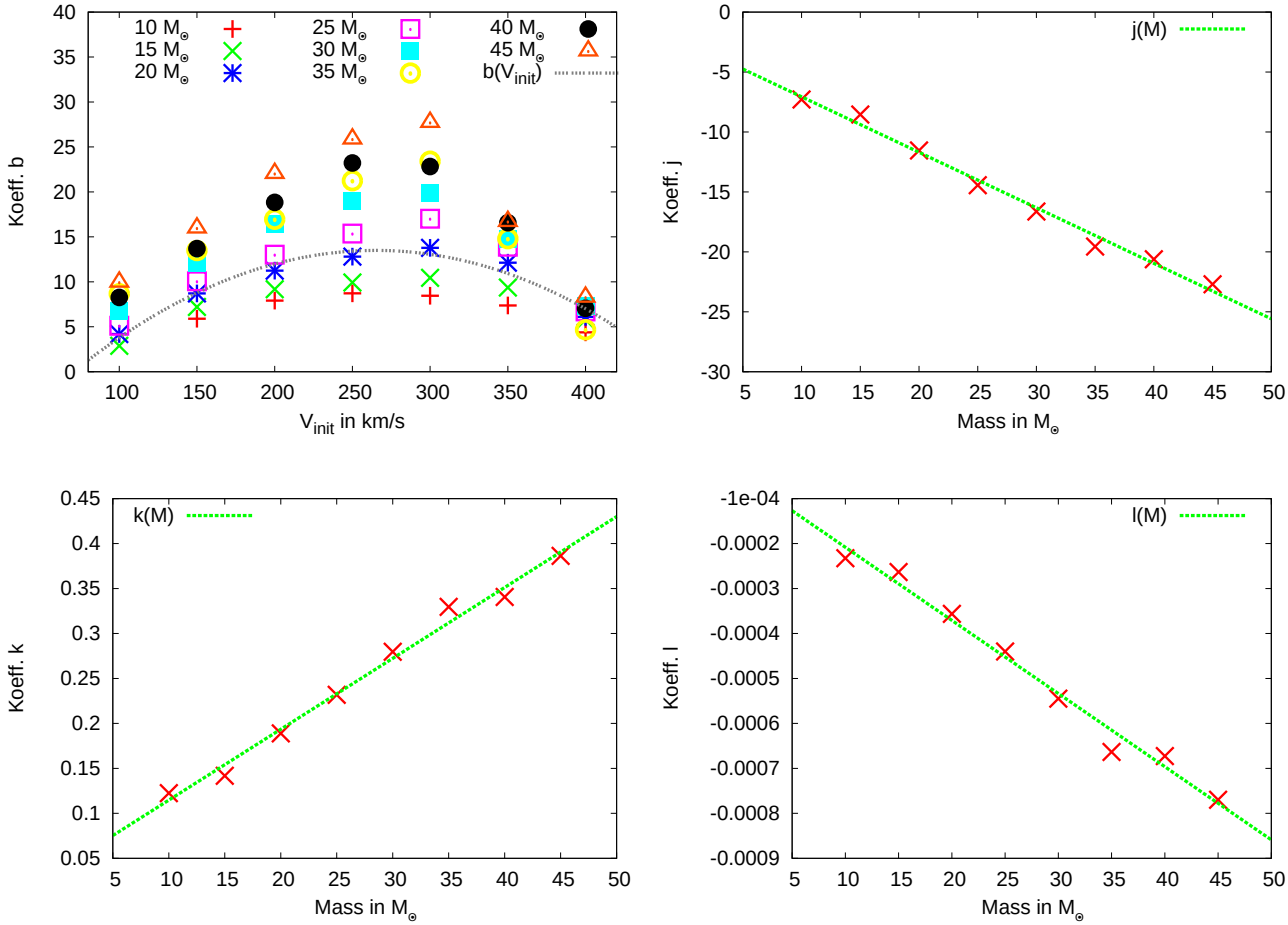

Figure 2: Parameterization of b from Eq.(1) for the example of the LMC grid. Upper left panel: Parameter b as function of $V_{\rm init}$ for different initial masses marked by different points written in the figure key. In dotted gray the equation $b = j + k \cdot \tau + l \cdot \tau^2$ is drawn fitted for the initial mass of $M = 20 M_{\odot}$. Other panels: Resulting values of j, k, l, respectively, from fitting parameter b as function of initial rotation velocity, as function of the initial mass of the model. In dotted green the linear approximation for $j(M), k(M), l(M)$ as function of initial mass, respectively.

Table 1: Range of initial rotation velocities and initial mass for which the derived equation for the nitrogen surface abundance are valid.

Galaxy	Mass in $M_\odot$	Rotational velocity in $\frac{\mathrm{km}}{\mathrm{s}}$
MW	$5-35$	$100-400$
LMC	$5-45$	$100-400$
SMC	$5-50$	$100-400$

Now Eq.(1) with two free parameters (b and c) is left which were determined by fitting the equation to the data of the stellar evolution grid. For this the fitting program GNUPLOT is used. The ranges for the initial mass and initial rotation velocity considered here for determining the dependence are presented in Tab.1. Higher initial masses and initial rotation velocities than shown in the Tab.1 were not included because these stellar models show a quasi chemically homogeneous evolution and a different behavior than in Fig.1 which can not be described by the $\gamma-$function.

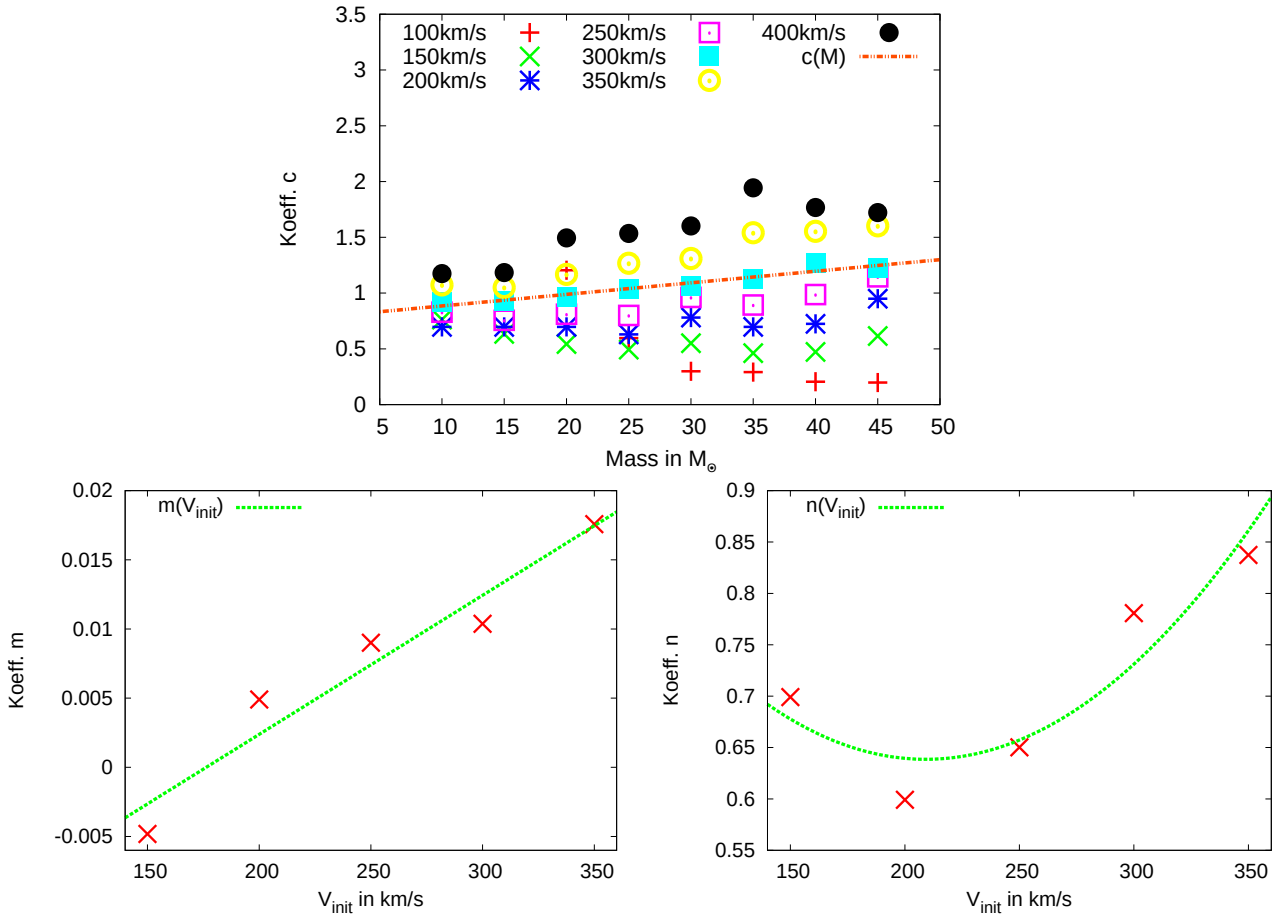

Figure 3: Parameterization of c from Eq.(1) for the example of the LMC grid. Upper left panel: Parameter c as function of initial mass for different initial rotation velocities marked by different points in the figure key. In dotted red the equation $c = m \cdot V_{\mathrm{init}} + n$ is drawn fitted for the initial rotation velocity of $V_{\mathrm{init}} = 300\frac{\mathrm{km}}{\mathrm{s}}$. Lower left panel: Resulting values of m from fitting parameter c as function of initial mass, as function of initial rotation velocity. In dotted green the linear approximation for $m(V_{\mathrm{init}})$ as function of initial rotation velocity. Lower right panel: Resulting values of n from fitting parameter c as function of initial mass, as function of initial rotation velocity. In dotted green the parabolic approximation for $n(V_{\mathrm{init}})$ as function of initial rotation velocity.

First, b as a function of the velocity is presented in Fig.2, which can be described by a polynomial of 2nd order: $b = j + k \cdot V_{\rm init} + l \cdot V_{\rm init}^2$. The new parameters j, k, l can be described as linear functions of mass. The result does depend on the metallicity so the parametrization has been done for the LMC, SMC and MW separately, and three different relations were obtained for b. For example, the result for the LMC is:

$$b(M[M_\odot], V_{\rm init}[\tfrac{\rm km}{\rm s}]) = -\frac{M+5.3}{2.2} + (M+4.6)\frac{V_{\rm init}}{127} + (M+2.8)\left(\frac{V_{\rm init}}{248}\right)^2. \quad (4)$$

For the parameter c the procedure is different. The dependence of c on the mass is presented in Fig.3, for which a linear function $c = n + m \cdot M$ is assumed. Then the new coefficients n, m are plotted against the rotation velocity. For n a parabola, and for m a linear function has been chosen. With this procedure the coefficient c was determined separately for the LMC, SMC and MW. For example, the result for the LMC is:

$$c(M[M_\odot], V_{\rm init}[\tfrac{\rm km}{\rm s}]) = \left(\frac{V_{\rm init}-180}{10000}\right) M + 0.64 + \left(\frac{V_{\rm init}-210}{300}\right)^2. \quad (5)$$

The complete list of fitting equations is given in Appendix B.

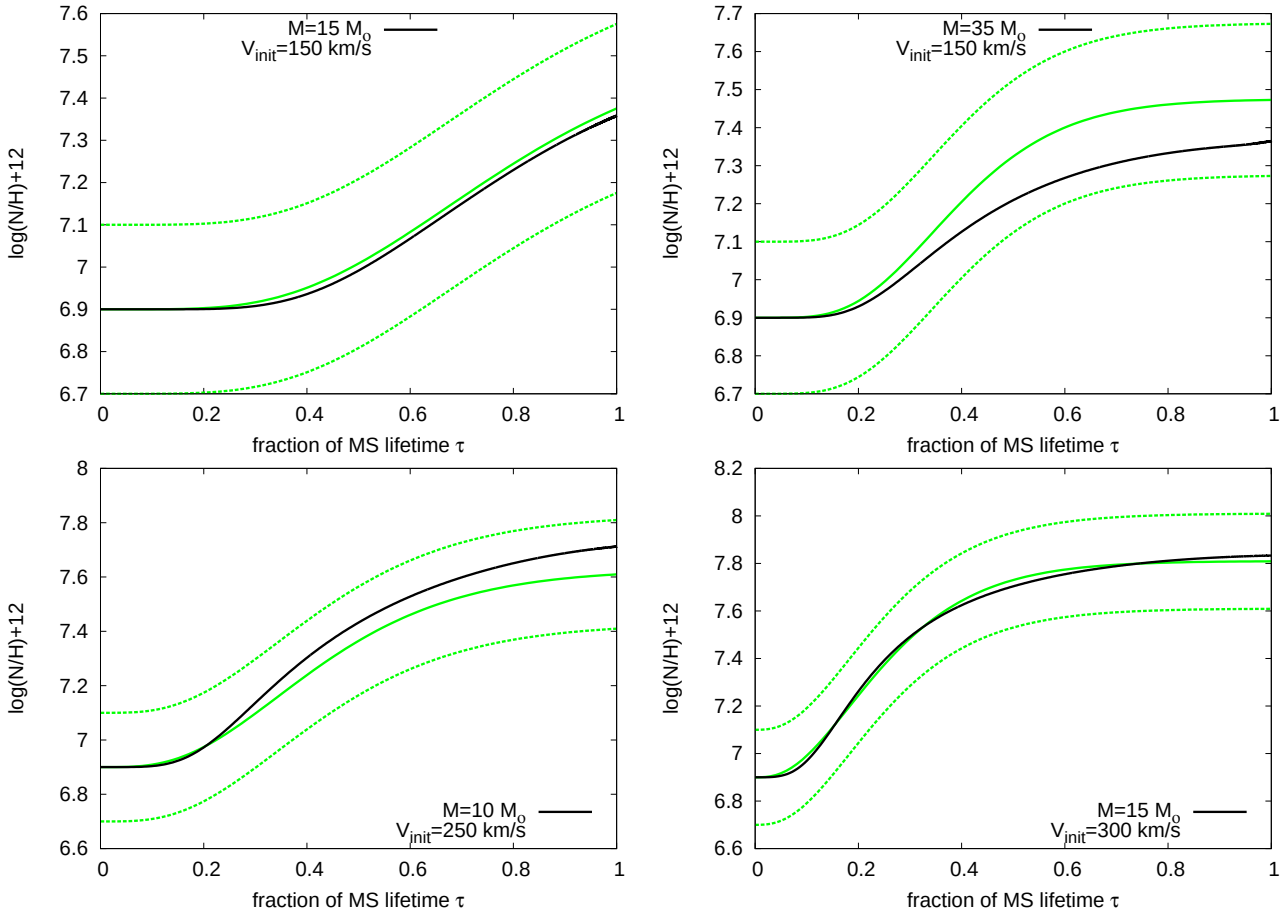

Figure 4: Examples for the discrepancy of the nitrogen surface abundance form the model grid data to the Eq.(1) with final setting of the parameters: Black solid line: surface nitrogen abundance evolution track from the model at LMC metallicity and initial values in the figure key. Green solid line: Eq.(1) with final set of the parameters to describe the nitrogen surface abundance as function of τ with the initial values given in the figure key. Green dotted line: solid green line with an offset of ± 0.2 dex, respectively, for an rough estimate of the discrepancy.

Obviously there is more than one way to do the parametrization of b and c. Many different possibilities have been tried and the procedure presented here provided the optimal compromise remaining between discrepancy to the grid data and compact resulting equations. In Fig.4, Eq.(1) with the above derived parametrization (in green) is confronted with nitrogen surface abundance evolution tracks of the model grid (in black), for selected initial masses and initial rotation velocities. For a rough estimate of the discrepancy between the evolution model tracks and the derived equations an offset of ± 0.2 dex, respectively, is added to the derived equation in the plots (dotted green lines). In the whole parameter range shown in Tab.1 the maximum discrepancy of the derived equation to the nitrogen surface abundance is less then the 0.2 dex. This is accurate enough to apply the derived equation to real observed data since the observational errors are usually 0.2 dex, or more. A general difference between the model and the derived equation is unavoidable if the equation should be of low order. The advantage of this low order function is, apart from the easy handling compared to for example a method based on interpolation on the stellar evolution grid, that the derived equations are smooth as function of initial rotation velocity and initial mass. The stellar models shows numerical anomalies how they can be seen in Fig.1, were the nitrogen abundance evolution tracks for the constant rotation velocity catch each other what is physically not expected. The derived equation anyway is smooth in rotation velocity and mass and therefore more physical.

2.2 The initial rotational velocity

A complete set of functions to describe the surface nitrogen abundance of stars with parameters in the range defined in Tab.1 was obtained. However note that the initial rotational velocity $V_{\rm init}$ is used in the equations of the parameters b, c and d. The initial rotational velocity $V_{\rm init}$ is not an observable quantity but it is the parameter of the simulations, the models are initialized with. The models are not initialized with hydrogen burning in the core but before, so when the models begin hydrogen burning in the core their rotation velocities already changed. To apply the results to observational data, a connection of the initial rotational velocity to the more physical relevant zero age main sequence (ZAMS) rotation velocity has to be derived.

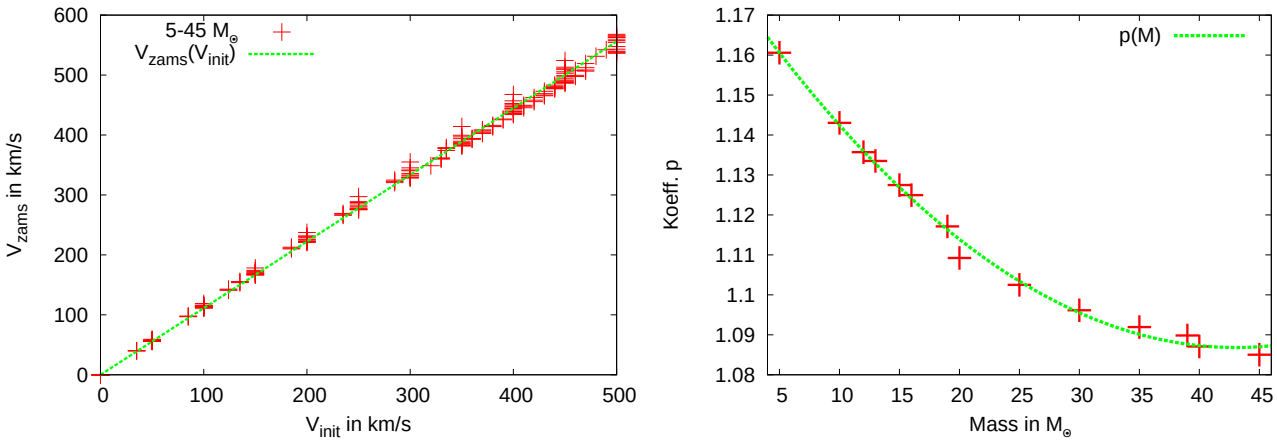

Figure 5: Left panel: ZAMS rotation velocity as function of the initial rotation velocity of the models of the stellar evolution grid at LMC metallicity in the initial mass range of $5 - 45 M_{\odot}$. The green dotted line is the fitted linear function $V_{ZAMS} = p \cdot V_{\rm init}$). Right panel: slope p as function of the initial mass of the models with a 2 nd order polynomial fitted as approximation for p as function of the initial mass.

In Fig.5 the initial versus the ZAMS rotational velocity is plotted. The velocities are proportional to each other by a factor p which is calculated by fitting a linear function $V_{\rm ZAMS} = p \cdot V_{\rm init}$ separately for the different initial masses of the grid models. So a mass dependent proportionality factor p is obtained. It also depends on the metallicity, so three different relations has been derived. For the LMC the relation is

$$V_{\rm ZAMS} = \left(1.18 - \frac{M}{228} - \left(\frac{M}{140}\right)^2\right) \cdot V_{\rm init}. \tag{6}$$

Now the ZAMS velocity can be calculated and the equations (8),(11) and (14) can be expressed as functions of the ZAMS rotation velocity, but we have to consider that a star may increase or decrease its rotational velocity during its life on the main sequence. Fig.6 shows how the surface rotational velocity of the stellar models behaves as a function of time and effective temperature for selected initial velocity and masses. Most of the main sequence lifetime, the rotation remains constant and then suddenly drops significantly. This happens due to a temperature drop at the surface of the star which leads to an effective loss of angular momentum due to an increased stellar wind. Since the surface rotation velocity is quite constant before, it is reasonable to use the ZAMS rotation velocity for the rotation velocity of the star for effective temperatures above 25000K.

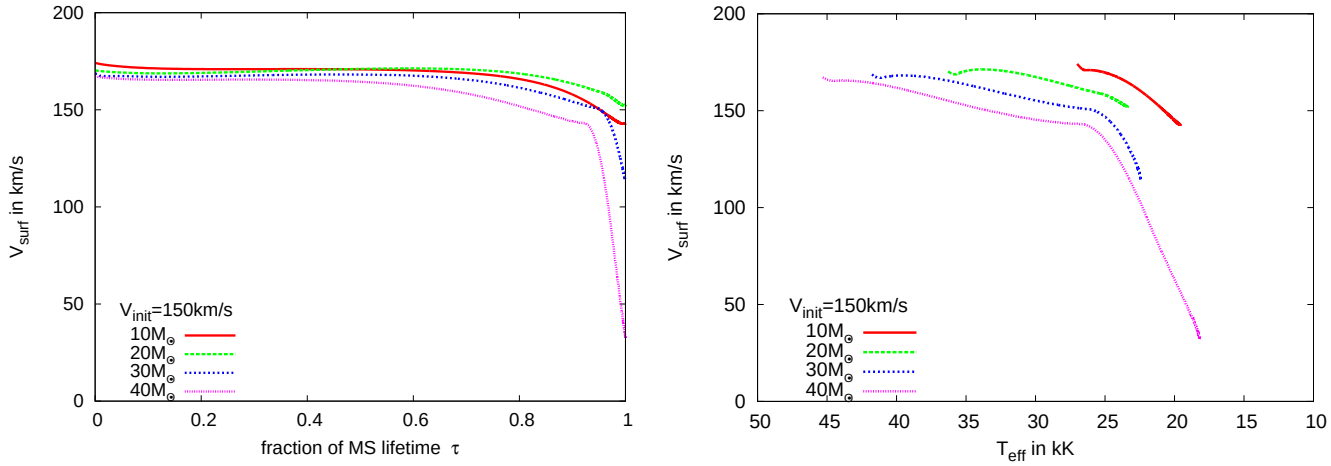

Figure 6: Evolution of the surface rotation velocity as function of time (left panel) and effective temperature (right panel) for models of the stellar grid at LMC metallicity for initial parameters given in the figure key.

2.3 Main sequence lifetime

Since equations that describe the nitrogen surface abundance as a function of the fraction of the MS lifetime were derived, the MS lifetime is a quantity required to be able to calculate absolute ages in Myr. It is extracted out of the stellar model grid data. The MS lifetime is a strong function of mass, but just week dependent on the rotational velocity. In Fig.7 the MS lifetime is shown on a double logarithmic scale with a fitted polynomial of 2nd order. For the purpose here it is enough to consider only the rotation velocity dependency as it is much stronger than the dependence on $V_{\rm init}$ for the MS lifetime. The MS lifetime depends also on the metallicity, so three relations, on each metallicity, were determined. The resulting equations are presented in App.B.

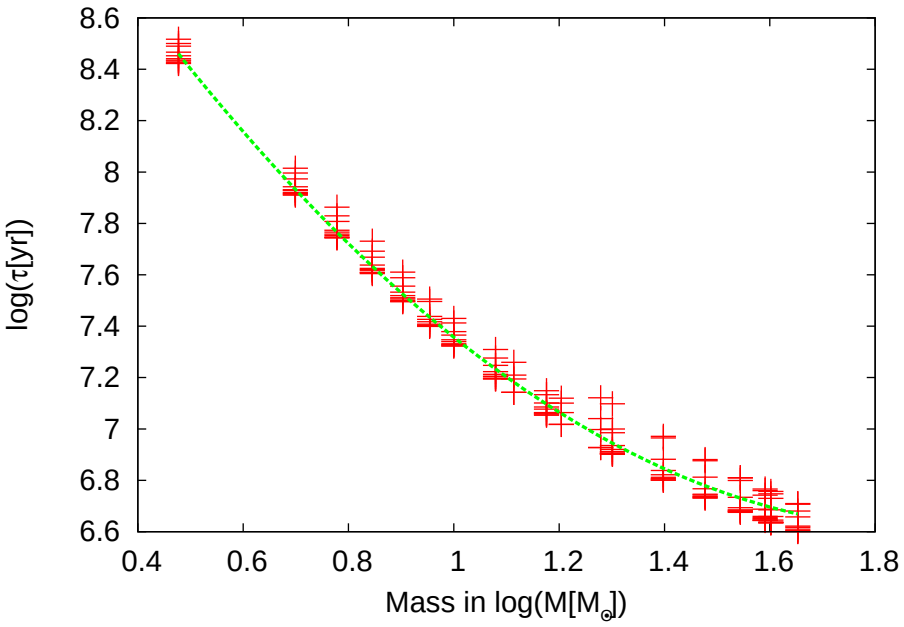

Figure 7: Main sequence lifetime τ as function of mass in a double logarithmic picture for models of the stellar grid with initial rotation velocities of $100 - 400 \frac{\mathrm{km}}{\mathrm{s}}$. The green dotted line is the fitted polynomial of 2 nd order to approximate τ as function of initial mass M.

3 VLT-FLAMES Observation Survey of Massive Stars

Recently a large spectroscopic survey of hot massive stars at the Very Large Telescope (VLT) of the European Southern Observatory (ESO) was performed. The aims of the survey were to learn about the chemical surface abundance in stars and the influence of the metallicity on the stellar wind. Therefore spectra of over 700 O and B-Type stars were obtained with the Fiber Large Array MulitElement Spectrograph (FLAMES). The stars are placed nearby clusters in the LMC (NGC2004 and N11 region), the SMC (NGC330 and NGC346) and the MW (NGC4755, NGC3293 and NGC6611). For detailed information on the observation see [Evans et al., 2005] and [Evans et al., 2006]. In previous work of [Hunter et al., 2008b] the atmospheric parameters, evolutionary masses and projected rotational velocities were evaluated using the non-LTE TLUSTY model atmosphere code applied to the spectra. The nitrogen absorption lines were used to derive the nitrogen surface abundance, or at least upper limits, of the sample stars, [Hunter et al., 2009]. To these resulting stellar properties, the equations derived (see Appendix B) can be applied to use the nitrogen abundance to derive ages for the observed stars. Since the equations have restrictions, a selection of stars from the FLAMES sample has been done as follows:

- available nitrogen abundance and atmospheric parameters,
- $V\sin(i) \geq 100\frac{\mathrm{km}}{\mathrm{s}}$,
- $T_{\mathrm{eff}} \geq 25000\mathrm{K}$.

In Sect.2.2 we argued that the stars have to have a high effective temperature ($\geq$ 25000K) to satisfy the approximation of applying the ZAMS rotation velocity for the current rotation velocity. The measured projected rotational velocity is a lower limit to the real velocity. Only stars with a high projected velocity ($\mathrm{Vsin}(i) \geq 100\frac{\mathrm{km}}{\mathrm{s}}$) were selected, to reject all stars that are nitrogen rich and intrinsically slowly rotating since these stars can not be explained with the theory of rotational mixing and are excluded from the sample [Hunter et al., 2008a].
Our selected sample contains in the end 50 stars, 27 LMC and 23 SMC stars.

3.1 Age constraints through nitrogen

The theory of rotational mixing is used to derive, through our equations in App.B, constraints on the age of the observed stars of our sample. To constrain the age it was searched for the time when the observed amount of nitrogen is obtained in the equations for the surface abundance (Eq.(8),(11),(14), respectively). The true rotation velocity of the star is required to obtain its age, which can not be obtained from the observations that only provide the projected rotational velocity $V\sin(i)$ and thus a lower limit to V. That means that only an upper limit for the stellar age could be derived since the rotation velocity can be larger and nitrogen can be mixed more efficient what leads to a lower age of the star. For the age constraint the observed stars had to be divided into two classes and to explain how the age is constrained examples for each class will be discussed in the next subsections.

3.1.1 Class 1 stars

The Class 1 is characterized by stars where the observed projected rotational velocity is high enough to reproduce the observed nitrogen amount with the equations in App.B. Fig.8 shows

how the age is determined for the LMC and Class 1 star N11-95, which has a measured mass of $M = 15\mathrm{M}_{\odot}$ and a $V\sin(i) = 267\frac{\mathrm{km}}{\mathrm{s}}$. The observed amount of nitrogen of N11-95 of $\mathcal{N} = 7.46$ is reached at $\tau = 0.498$. With a main sequence lifetime of $\tau_{\mathrm{MS}} = 9.2$ Myr, the maximum age of N11-95 is thus determined to 4.6 Myr. Additionally a curve for a rotation velocity of $V = 267\frac{\mathrm{km}}{\mathrm{s}} \cdot \frac{4}{\pi} = 340\frac{\mathrm{km}}{\mathrm{s}}$, were $\frac{4}{\pi}$ is the statistical correction factor for randomly distributed rotation axis of observed stars, is plotted in Fig.8. The age constraints from this higher velocity is much lower. It demonstrates why the constraint from the projected rotation velocity as an upper limit for the age needs to be taken. Taking a typical error on the measurement of the nitrogen surface abundance of 0.2 dex into account, an error from the calculations on the fraction of the main sequence lifetime of 0.2 was obtained, such that the typical error on the nitrogen age constraint is about 20%. If only an upper limit could be determined for the nitrogen surface abundance, the real abundance could be smaller which would lead to a lower maximum nitrogen age. In these cases the maximum nitrogen age is an upper limit, because of the projected rotational velocity and the upper limit nitrogen abundance, to the true age.

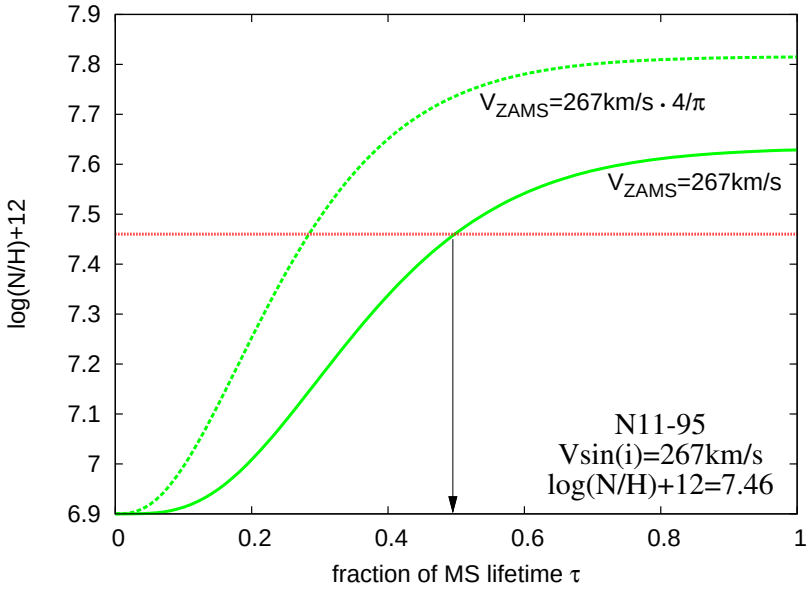

Figure 8: Age constraint for the LMC star N11-95. In red the observed level of nitrogen at the surface of this star is indicated. The green solid line shows the evolution of the nitrogen surface abundance calculated with the observed projected rotation velocity and Eq.(11). The green dashed line shows the evolution of the nitrogen surface abundance calculated with a rotation velocity of $V_{ZAMS} = 267\frac{\mathrm{km}}{\mathrm{s}} \cdot \frac{\pi}{4} = 340\frac{\mathrm{km}}{\mathrm{s}}$ with $\frac{\pi}{4}$ the statistical correction factor for randomly distributed rotational axis to th projected rotational velocity. The black arrow indicates the upper limit age constrain for N11-95 when the nitrogen abundance is reached by the green curve at $\tau = 0.498$.

3.1.2 Class 2 stars

The Class 2 is characterized by stars with nitrogen abundances that can not be explained by the measured projected rotational velocities with the equations in App.B. Fig.9 shows this case for the LMC and Class 2 star NGC2004-30. The nitrogen abundance curve from the Eq.(11), calculated with the projected rotation velocity $V\sin(i) = 123\frac{\mathrm{km}}{\mathrm{s}}$ and mass $M = 19\mathrm{M}_{\odot}$ of NGC2004-30, does not reach the observed nitrogen abundance measured $\mathcal{N} = 7.43$ during the whole main sequence lifetime. In these cases the minimum needed rotation velocity to explain the observed nitrogen surface abundance is calculated since the measured rotation velocity

is projected and can be higher. For NGC2004-30 the minimum needed rotation velocity is $V_{\rm min} = 164\frac{\rm km}{\rm s}$. Now it is possible to derive the minimum inclination angle $i_{\rm min}$ needed to get the minimum rotation velocity $V_{\rm min}$ with the relation

$$\sin(i_{\rm min}) = \frac{V\sin(i)}{V_{\rm min}} \ . \tag{7}$$

In case of NGC2004-30 the minimum inclination angle is $i_{\rm min} = 48.6°$. The maximum possible age of these stars is their main sequence lifetime, so it can not be constrained by the nitrogen abundance. The only information which can be obtained from Class 2 stars is the minimum inclination angle, which can be calculated with Eq.(7). If only an upper limit in the nitrogen abundance is available the true nitrogen level can be smaller and the minimum inclination angle would rise. If the true nitrogen abundance is much lower the star could become a Class 1 star.

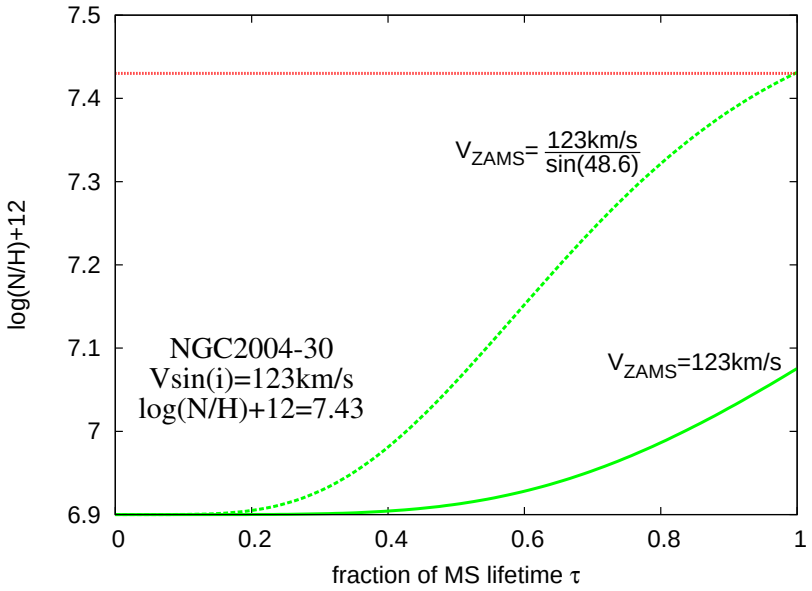

Figure 9: Constraint for the inclination angle of NGC2004-30. In red the observed level of observed nitrogen abundance of this star is indicated. The green solid line shows the evolution of the nitrogen surface abundance calculated with the observed projected rotation velocity and Eq.(11). The dotted green line is calculated with the minimum needed rotation velocity to reach the observed nitrogen abundance by adding an inclination angle of $i_{\rm min} = 48.6°$.

With the procedures presented above it is possible to derive a maximum nitrogen age constraint for the Class 1 stars and a minimum inclination angle for the Class 2 stars of the sample, except N11-84 because the measured nitrogen surface abundance is lower then the baseline abundance of the LMC. So this star is excluded in all further considerations.

3.1.3 Minimum inclination angle for Class 2 stars

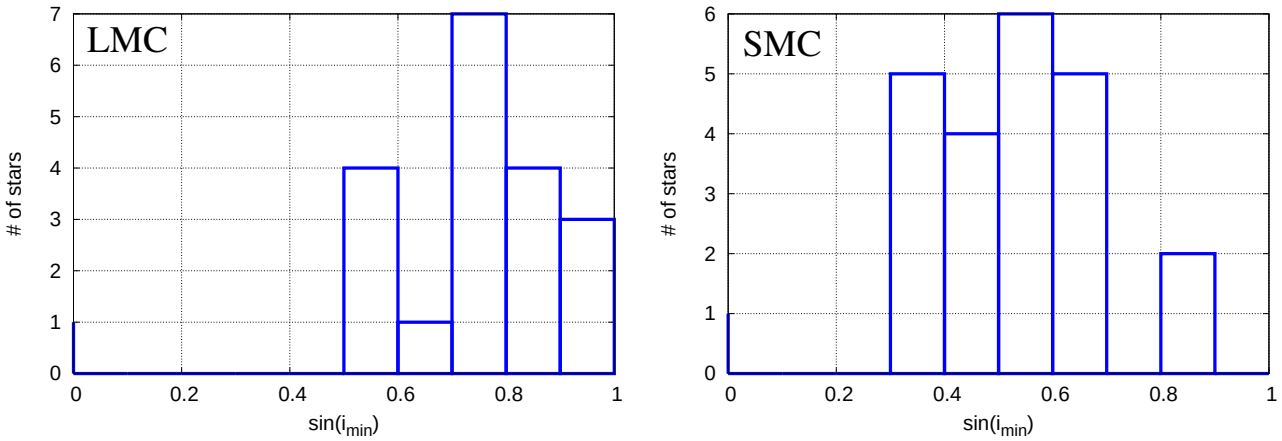

Figure 10: Minimum projection angle $\sin(i_{\rm min})$ needed for the LMC (left panel) and SMC (right panel) Class 2 stars so the rotation velocities of these stars are high enough to explain the measured nitrogen abundance on the surface.

With Eq.(7) the minimum inclination angle is calculated for Class 2 stars in the sample. A histogram for the minimum inclination angle is presented in Fig.10 for the LMC and SMC stars. We assume that the positions of the rotation axis of stars are randomly distributed, so if $\sin(i)$ is plotted the distribution should rise for higher values of $\sin(i)$. Since stars with small projected rotation velocities have been discarded from our sample also the small values of $\sin(i_{\rm min})$ were cut out. For the LMC, the figure shows the behavior expected within the low statistics of the sample, but not so for the SMC. In the SMC, $\sin(i_{\rm min}) \approx 0.5$ appears to be favored while higher values are rare. To explain the histogram of the SMC one needs to consider that for most of the SMC stars only an upper limit to the nitrogen abundance could be determined. In many cases, the upper limits might be well above the real abundance. This would explain why there is a favor for low values of $\sin(i_{\rm min})$ in the SMC.
In principle the minimum inclination angles can be used to test the rotational mixing. If the distribution of the angles follows the expectation it can be treated as indication supporting rotational mixing. But one has to be careful because in our SMC sample many stars have only an upper limit in the nitrogen abundance available which also effects the distribution if the upper limits are well above the true nitrogen surface abundance. If we would exclude all stars with only an upper limit in the abundance the number of stars is too low to make any statement out of the distribution of the $\sin(i_{\rm min})$.

3.2 Age estimates through isochrones in the Herzsprung-Russel-Diagram

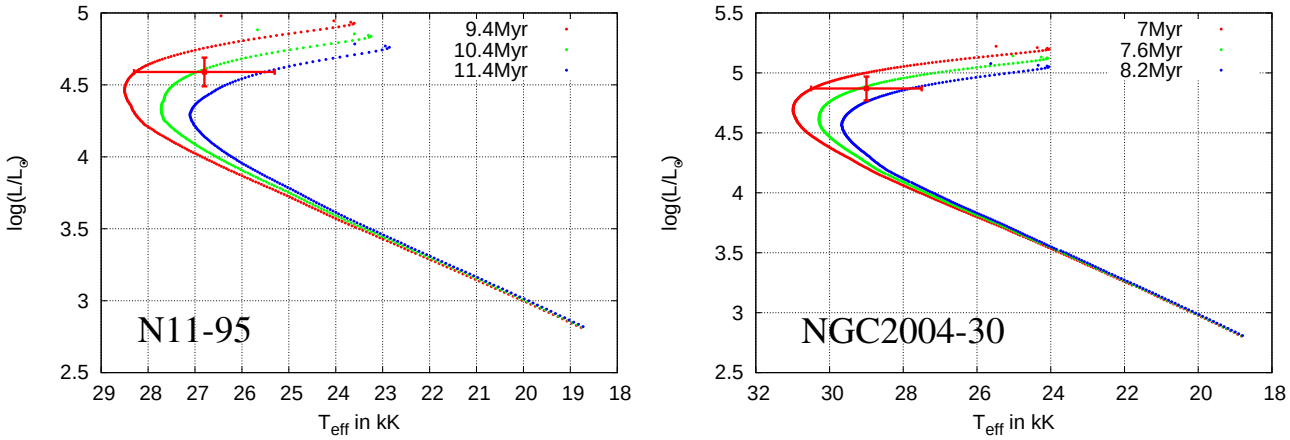

Figure 11: Hertzsprung-Russel-Diagram with the position of the LMC stars N11-95 (left panel) and NGC2004-30 (right panel) marked with the cross. In red, green and blue lines of equal age from the stellar evolution code are drawn for different ages given in the figure key. The green isochrone defines the age of the star while the red and blue one determines the maximum and minimum possible age, respectively, due to the uncertainties in measured temperature and luminosity of the LMC star.

For the Class 1 stars we could constrain the age with their nitrogen abundance and we want to compare this method with another age estimate that is believed to approximate the true age of stars well. Using the effective temperature and luminosity of the stars in our sample establishes the possibility to estimate their ages through their position in the Hertzsprung-Russell-Diagram. The stellar evolution grid was used to derive lines of equal age (isochrones) for nonrotating model stars in the HR diagram which goes up to 20Myr age with steps of 0.2Myr [Brott, I., private communication]. To each of the positions of the observed stars in the HR diagram an isochrone was fitted which defines the isochrone age of the star. So the age was estimated independent of the rotational mixing in the star. In Fig.11 the age constraints for N11-95 and NGC2004-30 are presented. Additionally isochrones were fitted for an error estimate due to the errors on the effective temperature of 1500K and on the luminosity of 0.1 dex, [Hunter et al., 2008b]. The error on the isochrone age was then determined to be ± 1 Myr in general.

4 Age comparison for Class 1 stars

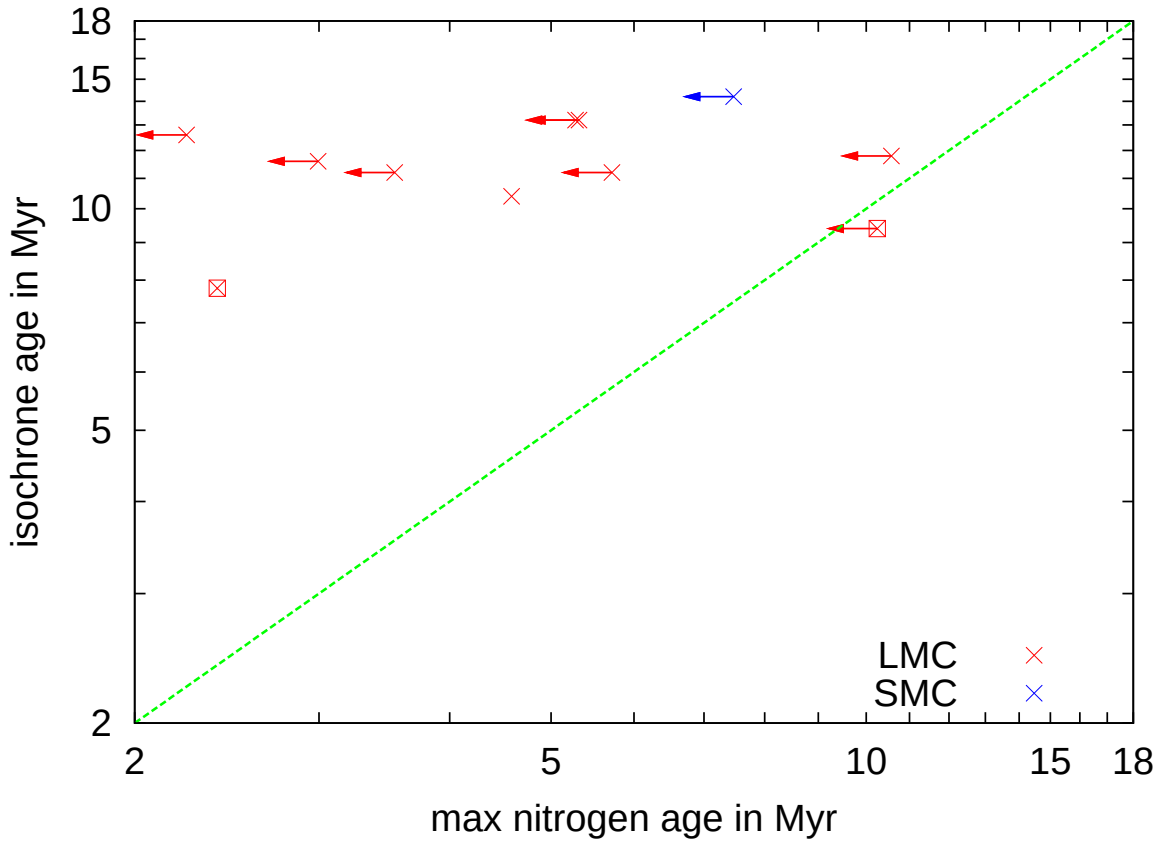

Figure 12: The age constraint from the measured nitrogen abundance plotted versus the age estimate from isochrones in the HR diagram for all Class 1 stars, LMC in red and SMC in blue. Stars with a measured upper limit in the nitrogen abundance are marked with an arrow. Discovered binaries in the sample are marked with a square.

In Fig.12 the maximum nitrogen age is plotted versus their isochrone age for all Class 1 stars of our sample. The Class 2 stars are excluded because we can not constrain their age using the nitrogen abundance. If only an upper limit in the nitrogen surface abundance for a measured star was available it is marked with an arrow. Discovered binaries are also marked with a square. The green dotted line in Fig.12 is the line of equal maximum nitrogen and isochrone age. The detailed numbers for each star are presented in Tab.2 in the App.A.
If the ages of the stars are predicted well with the theory of rotational mixing the expectation would be that all stars are placed below the green line of equal age in Fig.12, because just an upper limit for the nitrogen age could be determined. But in fact the picture obtained shows a different character. If all uncertainties are taken into account two stars, that are placed close to the line of equal age, are in agreement between the maximum nitrogen age and the isochrone age. The other nine stars of Class 1 have a low maximum nitrogen age compared with the isochrone age and have no agreement between the derived ages. The nitrogen surface abundance of these stars is lower then it should be to explain the isochrone age with the measured projected rotation velocity. It is easy to understand that the number of stars which are nitrogen poor and fast rotating have a higher probability to be detected in the Class 1 then nitrogen rich stars. Since the measured rotation velocity is a lower limit to the true rotation velocity, nitrogen rich stars will likely be Class 2 stars because even with a high projection angle i the high nitrogen amount can not be explained and the star will be

classified as Class 2. In contrast to that the nitrogen abundance in an unenriched and fast rotating star can be even explained with a low inclination angle i and the star remains in the Class 1. So the high fraction of stars that are in conflict with the age prediction through their nitrogen surface abundance is an effect of the method and that measured rotation velocities are lower limits to the true rotation. Another effect of the observation is that only one star in the Class 1 is placed in the SMC. Most stars in the SMC have just an upper limit in the nitrogen abundance available which may are well above the true abundance (Sect.3.1.3). Therefore most of the stars from the SMC belong to the Class 2 and just for one star the age could be constrained with the measured nitrogen surface abundance.

5 Conclusions

Through analyzing the evolution of the surface nitrogen abundance as function of time predicted by the theory of rotational mixing in single stars, a method to derive the age of a star due to its observed surface abundance in nitrogen, mass and rotational velocity has been presented. Since observations can only provide projected rotational velocities applying the method to observational data leads only to upper limits for the age. In Fig.12 the results of the new method described in this thesis are compared with stellar ages derived from isochrones in the HR diagram (see Sec.4). A group of nitrogen poor and fast rotating stars could be identified which are in conflict with the age predicted through the measured nitrogen surface abundance. For further considerations the sample of stars is too small and the amount of stars that have only an upper limit is to high.
In previous work of [Brott et al., 2010b] the VLT-FLAMES survey of the LMC was compared with a synthetic star population, based on the same stellar grid used here, for the LMC sample. They also found a group of nitrogen unenriched and fast rotating stars which contains the same stars as the group of stars that are in conflict with their age presented here. In this thesis the result of the nitrogen poor and fast rotating stars being inconsistent with the theory of rotational mixing could be confirmed by independent considerations: their nitrogen age was found to be systematically much smaller that their isochrone age.
A possibility to explain a population of nitrogen poor and fast rotating stars is binary evolution with interaction of stars, although only one of nine stars that are in conflict with the theory of rotational mixing in this thesis is discovered as binary, since post-interacting binaries may not be classified as binary. Therefore interaction of stars as origin for the nitrogen poor and fast rotating stars can not be excluded. Special attention to binaries and is given in the upcoming VLT-FLAMES Tarantula survey, [Evans et al., 2010], which may determine the role of binaries in the chemical evolution of stars.
A new method for testing the theory of rotational induced mixing has been presented which provides a comparison for each star of an age constraint through the nitrogen abundance with an age estimate due to isochrones in the HR diagram. With this mehtod the theory of rotational mixing can be directly tested through a stellar evolution grid without making further assumptions, i. e. the stellar formation history of a stellar population. The method is suitable for detecting peculiar abundances in stars with low a complexity. Therefore this new method presented in this thesis is very promising to test the theory of rotational mixing.

References

[Brott et al., 2010a] Brott I., Langer N. & de Koter, 2010, A&A in preperation

[Brott et al., 2010b] Brott I., Evans C., Hunter I. et al., *A Quantitative Test of the Theory of Rotational Mixing in Massive Stars*, in preperation

[Dufton et al., 2006] Dulfton P.L., Smartt S.J., Lee J.K. et al., 2006, *The VLT-FLAMES survey of massive stars: stellar parameters and rotational velocities in NGC3293, NGC4755 and NGC6611*, A&A 457 265

[Endal & Sofia, 1976] Endal A.S. & Sofia S., 1976, *The evolution of rotating stars. I. Method and exploratory calculations on a $7M_{\odot}$ star*, ApJ 210 184E

[Endal & Sofia, 1978] Endal A.S. & Sofia S., 1978, *The evolution of rotating stars. II. Calculations with time-dependent redistribution on angular momentum for $7M_{\odot}$ and $10M_{\odot}$ stars.*, ApJ 220 279E

[Evans et al., 2005] Evans C.J., Smartt S.J., Lee J.K. et al., 2005, *The VLT-FLAMES survey of massive stars: Observations in the Galactic clusters NGC3293, NGC4755 and NGC6611*, A&A 437 467

[Evans et al., 2006] Evans C.J., Lennon D.J., Smartt S.J. & Trundle C., 2006, *The VLT-FLAMES survey of massive stars: observations centered on the Magellanic Cloud clusters NGC330, NGC346, NGC2004, and the N11 region*, A&A 456 623

[Evans et al., 2010] Evans C.J., Bastian N., Beletsky Y. et al., 2010, *The VLTFLAMES Tarantula Survey*, IAU Symposium No. 266, 35-40

[Haiman & Loeb, 1997] Haiman Z. & Loeb A., 1997, *Signatures of stellar reionization of the universe*, ApJ 483 21H

[Hunter et al., 2008a] Hunter I., Brott I., Lennon D.J. et al., 2008, *The VLT FLAMES Survey of Massive Stars: Rotation and Nitrogen Enrichment as the Key to Understanding Massive Star Evolution*, ApJ 676 L29

[Hunter et al., 2008b] Hunter I., Lennon D.J., Dulfton P.L. et al., 2008, *The VLT-FLAMES survey of massive stars: atmospheric parameters and rotational velocity distributions for B-type stars in the Magellanic Clouds*, A&A 479 541

[Hunter et al., 2009] Hunter I., Brott I., Langer N. et al., 2009, *The VLT-FLAMES survey of massive stars: constraints on stellar evolution from the chemical compositions of rapidly rotating Galactic and Magellanic Cloud B-type stars*, A&A 496 841

[Pols 2009] Pols O.R., 2009, *Stellar structure and evolution*, lecture notes on an advanced astrophysics course on Stellar Structure and Evolution given at Utrecht University

[Yoon et al., 2006] Yoon S.-C., Langer N. & Norman C., 2006, *Single star progenitors of long gamma-ray bursts 1. Model grids and redshift dependent GRB rate*, A&A 460 199

[Heger & Langer, 2000] Heger A. & Langer N., 2000, *Presupernova evolution of rotating massive stars. II. evolution of the surface properties*, ApJ 544 1016

Appendix A

Table 2: List of stars with their properties; atmospheric parameters, nitrogen surface abundance, rotation velocity and binary from [Hunter et al., 2009] and [Hunter et al., 2008b]; $\sin(i_{\min})$, maximum nitrogen and isochrone age are results of this thesis.

Star	$V \sin(i)$ in $\frac{\text{km}}{\text{s}}$	T_{eff} in K	$M_{\text{evol.}}$ in $M_\odot$	nitrogen surface abundance in dex	MS lifetime in Myr	$\sin(i_{\min})$	max nitrogen age in Myr	isochrone age in Myr	binary	Class
NGC346-27	220	31000	18	<7.71	6.6	0.56	6.6	7.6		2
NGC346-32	125	29000	17	<6.88	8.6	0.86	8.6	9.2	√	2
NGC346-53	170	29500	15	<7.44	9.0	0.56	9.0	9.4	√	2
NGC346-55	130	29500	15	<7.25	9.7	0.63	9.7	9.4		2
NGC346-58	180	29500	14	<7.56	9.5	0.49	9.5	9.6	√	2
NGC346-70	109	30500	15	<7.50	8.9	0.33	8.9	8.2		2
NGC346-79	293	29500	14	<7.88	8.9	0.64	8.9	9.4		2
NGC346-80	216	27300	12	<7.85	11.4	0.47	11.4	12.8		2
NGC346-83	207	27300	12	<7.73	11.7	0.48	11.7	12.8	√	2
NGC346-84	105	27300	12	<7.06	13.8	0.59	13.8	12.8		2
NGC346-92	234	27300	12	<7.52	12.3	0.67	12.3	12.8		2
NGC346-100	183	26100	11	<7.41	14.6	0.60	14.6	15.0		2
NGC346-106	142	27500	12	<7.51	12.3	0.41	12.3	12.4	√	2
NGC346-108	167	26100	11	<7.42	14.6	0.54	14.6	15.0		2
NGC346-109	123	26100	11	<7.09	15.8	0.66	15.8	15.0		2
NGC346-114	287	27300	12	<7.80	11.5	0.64	11.5	12.6		2
NGC330-21	204	30500	21	<7.64	5.6	0.57	5.6	7.0		2
NGC330-38	150	27300	14	<7.16	10.9	0.80	10.9	11.2		2
NGC330-39	120	33000	18	<7.61	6.8	0.34	6.8	6.4		2
NGC330-41	127	32000	17	7.73	7.1	0.32	7.1	7.2		2
NGC330-51	273	26100	12	<7.20	12.9	1.00	7.5	14.2		1
NGC330-57	104	29000	13	<7.48	11.0	0.32	11.0	10.2		2
NGC330-97	154	27300	11	7.60	13.8	0.40	13.8	12.0		2

Star	$V \sin(i)$ in $\frac{\text{km}}{\text{s}}$	T_{eff} in K	$M_{\text{evol.}}$ in $M_\odot$	nitrogen surface abundance in dex	MS lifetime in Myr	$\sin(i_{\min})$	max nitrogen age in Myr	isochrone age in Myr	binary	Class
N11-34	203	25500	20	7.12	6.6	1.00	2.4	7.8	√	1
N11-37	100	28100	23	<7.17	6.1	0.81	6.1	6.8	√	2
N11-46	205	33500	28	<7.71	4.4	0.79	4.4	4.8	√	2
N11-84	108	29500	18	<6.89	8.2	–	–	8.0	√	–
N11-88	240	24150	14	<6.96	10.4	1.00	2.2	12.6		1
N11-95	267	26800	15	7.46	9.2	1.00	4.6	10.4		1
N11-102	218	31000	18	<7.58	7.4	0.95	7.4	7.0		2
N11-104	153	25700	14	<7.20	11.1	1.00	10.6	11.8		1
N11-114	299	32500	19	<7.92	6.3	0.85	6.3	5.8		2
N11-117	247	26800	13	<7.06	11.5	1.00	3.5	11.2		1
N11-118	150	25700	13	7.39	12.1	0.82	12.1	12.6	√	2
N11-120	207	31500	17	<7.56	8.0	0.93	8.0	6.4		2
N11-121	265	27000	14	<7.48	10.2	1.00	5.7	11.2		2
N11-122	173	33000	18	<7.72	7.0	0.59	7.0	4.6		2
NGC2004-30	123	29000	19	7.43	7.3	0.75	7.3	7.6	√	2
NGC2004-62	106	31750	17	<7.33	8.5	0.68	8.5	7.6		2
NGC2004-66	238	25700	13	7.98	10.4	0.60	10.4	12.0		2
NGC2004-69	178	28000	15	7.84	8.7	0.51	8.7	9.8		2
NGC2004-74	130	27375	14	<7.42	10.8	0.71	10.8	10.6	√	2
NGC2004-77	215	29500	16	7.65	8.4	0.79	8.4	8.4		2
NGC2004-81	105	26800	13	7.14	12.4	0.71	12.4	11.2		2
NGC2004-82	161	25700	13	7.47	11.9	0.80	11.9	12.6		2
NGC2004-95	138	25700	13	7.13	12.4	0.95	12.4	12.8		2
NGC2004-100	323	26800	13	<7.29	10.9	1.00	3.0	11.6		1
NGC2004-104	274	25700	12	<7.28	12.8	1.00	5.2	13.2		1
NGC2004-105	235	25700	12	<7.11	13.2	1.00	5.3	13.2		1
NGC2004-107	146	28500	14	<7.12	11.1	1.00	10.2	9.4	√	1

Appendix B

In this section the resulting relations for the three different metallicities (MW,LMC,SMC) are presented. The equations are calculated as described in Sect.2 and are used in this form for all calculations in Sect.3 and Sect4.

Milky Way

The nitrogen surface abundance for massive stars in the Solar neighborhood can be described by

$$\mathcal{N}(\tau) = a + c \cdot \gamma_d(b \cdot \tau) \tag{8}$$

where

$$\begin{aligned} a &= 7.64, \\ d &= 9 - \tfrac{V_{\rm init}}{50}, \\ b &= -\tfrac{M+2.2}{4.54} + (M+12.4)\tfrac{V_{\rm init}}{210.4} - (M+13.9)\left(\tfrac{V_{\rm init}}{340.8}\right)^2, \\ c &= 0.4 + \left(\tfrac{V_{\rm init}-245.5}{16826}\right) + \left(\tfrac{V_{\rm init}-252}{280}\right)^2, \end{aligned}$$

with M in $\mathrm{M}_\odot$ and $V_{\rm init}$ in $\frac{\rm km}{\rm s}$. For the ZAMS velocity

$$V_{\rm ZAMS} = \left(1.13 - \tfrac{M}{263} + \left(\tfrac{M}{170}\right)^2\right) \cdot V_{\rm init} \tag{9}$$

was obtained and the main sequence lifetime can be expressed as

$$\lg\left(\tfrac{\tau}{\rm yr}\right) = 10.07 - 3.66 \cdot \lg\left(\tfrac{M}{\mathrm{M}_\odot}\right) + 0.97 \cdot \left(\lg\left(\tfrac{M}{\mathrm{M}_\odot}\right)\right)^2. \tag{10}$$

Large Magellanic Cloud

The nitrogen surface abundace for massive stars in the Large Magellanic Cloud can be described by

$$\mathcal{N}(\tau) = a + c \cdot \gamma_d(b \cdot \tau) \tag{11}$$

where

$$\begin{aligned} a &= 6.9, \\ d &= 9 - \tfrac{V_{\rm init}}{50}, \\ b &= -\tfrac{M+5.3}{2.2} + (M+4.6)\tfrac{V_{\rm init}}{127} - (M+2.8)\left(\tfrac{V_{\rm init}}{248}\right)^2, \\ c &= 0.64 + \left(\tfrac{V_{\rm init}-180}{10000}\right) + \left(\tfrac{V_{\rm init}-210}{300}\right)^2, \end{aligned}$$

with M in $\mathrm{M}_\odot$ and $V_{\rm init}$ in $\frac{\rm km}{\rm s}$. For the ZAMS velocity

$$V_{\rm ZAMS} = \left(1.18 - \tfrac{M}{228} + \left(\tfrac{M}{140}\right)^2\right) \cdot V_{\rm init} \tag{12}$$

was obtained and the main sequence lifetime can be expressed as

$$\lg\left(\tfrac{\tau}{\rm yr}\right) = 9.90 - 3.44 \cdot \lg\left(\tfrac{M}{\mathrm{M}_\odot}\right) + 0.90 \cdot \left(\lg\left(\tfrac{M}{\mathrm{M}_\odot}\right)\right)^2. \tag{13}$$

Small Magellanic Cloud

The nitrogen surface aboundace for massive stars in the Small Magellanic Cloud can be described by

$$\mathcal{N}(\tau) = a + c \cdot \gamma_d(b \cdot \tau) \tag{14}$$

where

$$\begin{aligned} a &= 7.64, \\ d &= 9 - \tfrac{V_{\rm init}}{50}, \\ b &= -\tfrac{M+1.1}{1.5} + (M+4.5)\tfrac{V_{\rm init}}{111} - (M+3.8)\left(\tfrac{V_{\rm init}}{236}\right)^2, \\ c &= 0.8 + \left(\tfrac{V_{\rm init}-180}{11988}\right) + \left(\tfrac{V_{\rm init}-180}{360}\right)^2, \end{aligned}$$

with M in $\mathrm{M}_\odot$ and $V_{\rm init}$ in $\frac{\rm km}{\rm s}$. For the ZAMS velocity

$$V_{\rm ZAMS} = \left(1.22 - \tfrac{M}{270} + \left(\tfrac{M}{158}\right)^2\right) \cdot V_{\rm init} \tag{15}$$

was obtained and the main sequence lifetime can be expressed as

$$\lg\left(\tfrac{\tau}{\rm yr}\right) = 9.80 - 3.28 \cdot \lg\left(\tfrac{M}{\mathrm{M}_\odot}\right) + 0.82 \cdot \left(\lg\left(\tfrac{M}{\mathrm{M}_\odot}\right)\right)^2. \tag{16}$$

Ich versichere, dass ich diese Arbeit selbständig verfasst und keine anderen als die angegebenen Quellen und Hilfsmittel benutzt sowie die Zitate kenntlich gemacht habe.

Bonn, den Unterschrift